Electronic Supplementary Information

Experimental Section

Materials: NH_4F, KH_2PO_4, K_2HPO_4 and urea were purchased from Beijing Chemical Corp. $Co(NO_3)_2 \cdot 6H_2O$ was purchased from Aladdin Ltd (China). Ti mesh was purchased from Hangxu filter flagship store. Pt/C (10 wt% Pt) was purchased from Alfa Aesar (China) Chemicals Co. Ltd. $RuCl_3 \cdot 3H_2O$ and Nafion (5 wt%) were purchased from Sigma-Aldrich Chemical Reagent Co. Ltd. All the reagents were used as received without further purification. The water used throughout all experiments was purified through a Millipore system.

Preparation of Co(OH)F/TM: Co(OH)F was prepared as follows. In a typical synthesis, $Co(NO_3)_2 \cdot 6H_2O$ (1 mmol), NH_4F (2 mmol) and urea (5 mmol) were dissolved in 25 mL water under vigorous stirring for 20 min. Then the solution was transferred into a Teflon-lined stainless autoclave (30 mL), and a piece of Ti mesh (3 cm × 2 cm) was immersed into the autoclave contained solution. The autoclave was sealed and maintained at 105 °C for 5 h in an electric oven. After the autoclave cooled down naturally, the resulting Co(OH)F/TM was taken out and washed with ultrapure water and dried at 60 °C.

Preparation of Co_2N/TM: To prepare Co_2N/TM, Co(OH)F/TM was placed in the furnace and heated to 420 °C for 2 h with a heating speed of 5 °C min^{-1} under a flowing NH_3 atmosphere. The system was allowed to cool down to room temperature naturally still under a flowing NH_3 atmosphere. Finally, the black Co_2N/Ti was collected for further characterization. The loading for Co_2N on Ti mesh was determined to be 1.08 mg cm^{-2}.

Preparation of Co-Pi/TM: The Co-Pi/TM was formed with a rapid electrochemical transformation. Co_2N /TM electrode (0.5 × 0.5 cm) was used as the working electrode, Pt wire as the auxiliary electrode and SCE electrode as the reference electrode. the as-prepared Co_2N/TM was activated for 500 cycles by cyclic voltammetry with the potential ranges from 0.8 V to 1.2 V vs. SCE in 0.1 M PBS at pH 7.4.

Preparation of RuO_2: RuO_2 was prepared according to previous report.[1] Briefly,

2.61 g $RuCl_3 \cdot 3H_2O$ and 1.0 mL NaOH (1.0 M) were added into 100 mL distilled water and stirred for 45 min at 100 °C. Then the solution was centrifuged for 10 minutes and filtered. The precipitate was collected and washed with water several times. Finally, the product was dried at 80 °C overnight and then annealed at 300 °C in air for 3 h.

Characterizations: XRD data were collected on a Rigaku X-ray diffractometer equipped with a Cu Kα radiation source. Scanning electron microscopy (SEM) measurements were performed on a Hitachi S-4800 field emission scanning electron microscope at an accelerating voltage of 20 kV. Transmission electron microscopy (TEM) measurements were carried out on a Zeiss Libra 200FE transmission electron microscope operated at 200 kV. X-ray photoelectron spectroscopy (XPS) measurements were performed on an ESCALABMK II X-ray photoelectron spectrometer using Mg as the exciting source. ICP-MS analysis was performed on ThermoScientific iCAP6300.

Electrochemical measurements: Electrochemical measurements were performed with a CHI 660E electrochemical analyzer (CH Instruments, Inc., Shanghai) in a standard three-electrode system, using a Co-Pi/TM as the working electrode, a Pt wire as the counter electrode and a SCE as the reference electrode. The potentials reported in this work were calibrated to RHE, using the following equation: E (RHE) = E (SCE) + 0.242 + 0.059 × pH V. Polarization curves were obtained using linear sweep voltammetry with a scan rate of 2 mV s^{-1}. All experiments were carried out at room temperature (~25 °C).

Computational Methods: All the density-functional theory (DFT) calculations in this study were performed using the Vienna *ab initio* simulation package (VASP).[2-4] We used the PBE functional for the exchange-correlation energy[5] and projector augmented wave (PAW) potentials.[6,7] The kinetic energy cutoff in the calculation was set to 450 eV. The ionic relaxation was performed until the force on each atom is less than 0.03 eV/Å and convergence criteria of total energy were set to 10^{-4} eV. The 3×3×1 k-points meshes were sampled based on the Monkhorst-Pack method. [8] The Hubbard U parameter (GGA+U) with U = 4 eV was used to calculate the electron

correlation within the Co ions. The simulations performed were based on the five-layer thick $Co_2N(111)$ surface and a Co-Pi layer model structure with H atoms to saturate the dangling bonds of O atoms.[9] To minimize the undesired interactions between images, a vacuum of at least 15 Å was considered along the z axis.

Previous studies have shown that the OER activity is strongly correlated with the free energy of O*, OH* and OOH* binding to the electrocatalysts surface. The four step OER mechanism is proposed as:

$$2H_2O + * \rightarrow OH^* + H_2O + e^- + H^+ \quad (1)$$

$$OH^* + H_2O \rightarrow O^* + H_2O + e^- + H^+ \quad (2)$$

$$O^* + H_2O \rightarrow OOH^* + e^- + H^+ \quad (3)$$

$$OOH^* \rightarrow O_2 + e^- + H^+ \quad (4)$$

The free energy (ΔG_i) for O*, OH* and OOH* adsorption on Co-Pi and surfaces was calculated as follows:

$$\Delta G_i = \Delta E_i + \Delta E_{ZPE} - T\Delta S \quad (5)$$

where ΔE_i is the reaction energy for each elementary step, ΔE_{ZPE} is the zero-point energy change and ΔS is the entropy change. The theoretical overpotential can be defined as:

$$\eta = \max[\Delta G_1, \Delta G_2, \Delta G_3, \Delta G_4]/e - 1.23\ [V] \quad (6)$$

Determination of Faradaic efficiency (FE): The generated gas was confirmed by gas chromatography (GC) analysis and measured quantitatively using a calibrated pressure sensor to monitor the change of pressure in the anode and cathode compartment of a H-type electrolytic cell. The FE was calculated by comparing the amount of experimentally quantified gas with theoretically calculated (assuming 100% FE). GC analysis was carried out on GC-2014C with thermal conductivity detector and nitrogen carrier gas. Pressure data during electrolysis were recorded using a CEM DT-8890 Differential Air Pressure Gauge Manometer Data Logger Meter Tester with a sampling interval of 1 point per second.

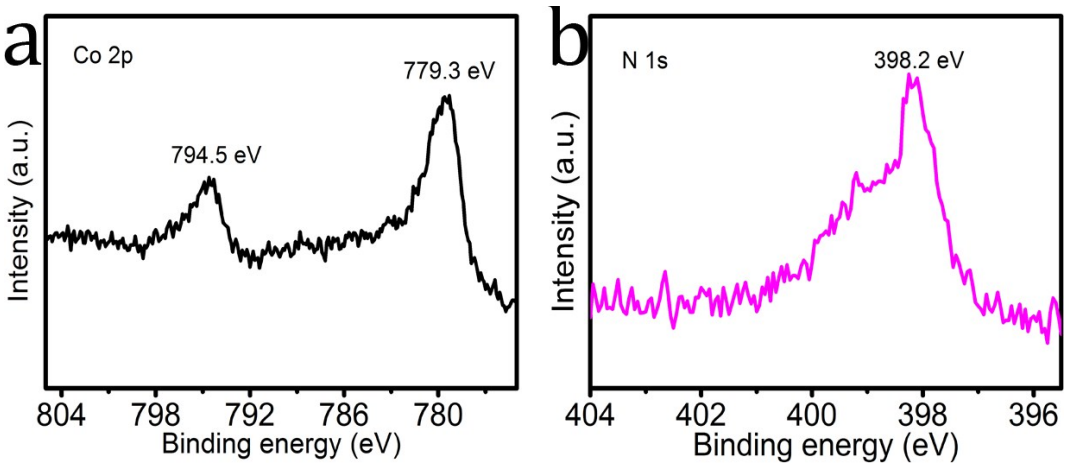

Fig. S1. XPS spectra of Co_2N in (a) Co 2p, and (b) N 1s regions.

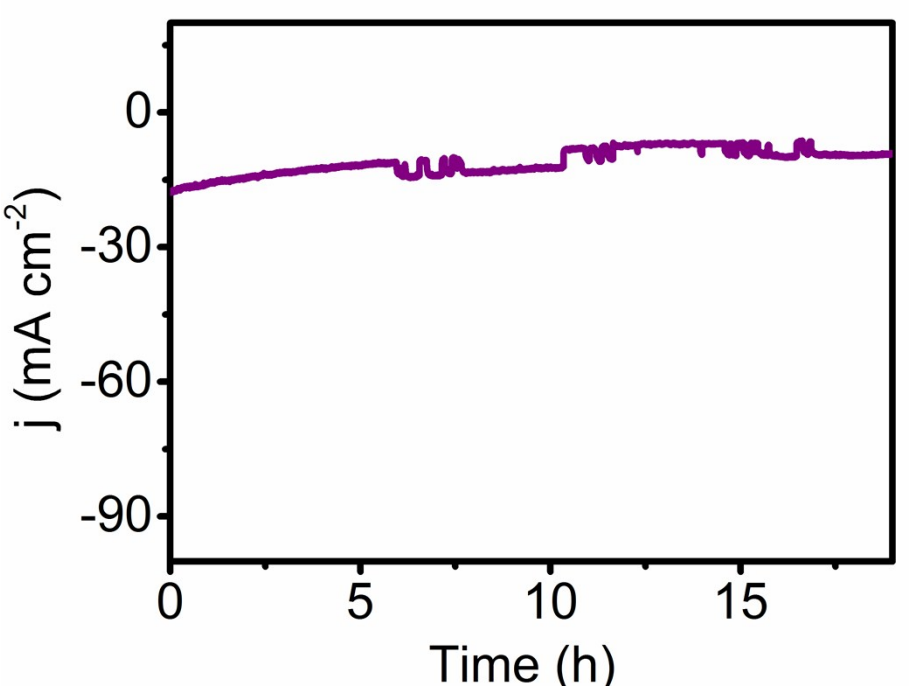

Fig. S2. Time-dependent current density curve of Pt/C under static overpotential in 1.0 M PBS.

Table S1. Comparison of HER performance for Co_2N/TM with other non-noble-metal electrocatalysts in neutral media.

Catalyst	j (mA cm^{-2})	η (mV)	Electrolyte	Ref.
Co_2N/TM	2	142	1.0 M PBS	This work
	5	246		
	10	290		
WO_3 NAs/CC	2	186	1.0 M PBS	10
	10	302		
CoO/$CoSe_2$	10	337	0.5 M PBS	11
H_2-CoCat/FTO	2	385	0.5 M PBS	12
$CuMoS_4$/FTO	2	210	0.1 M PBS	13
Cu-EA	2	270	0.1 M PBS	14
Co-NRCNTs	2	380	0.1 M PBS	15
	10	540		
Co-Mo-S film	1.04	200	PBS	16
Mo_2C	1	200	PBS	17
CoP/CC	2	65	1.0 M PBS	18
	10	106		

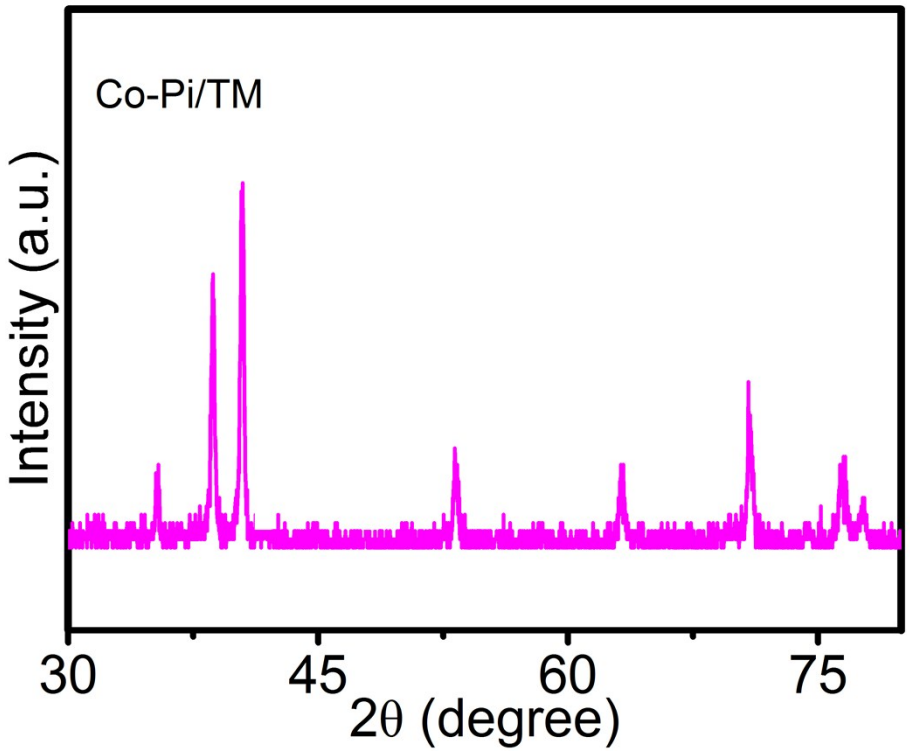

Fig. S3. XRD pattern for Co-Pi/TM.

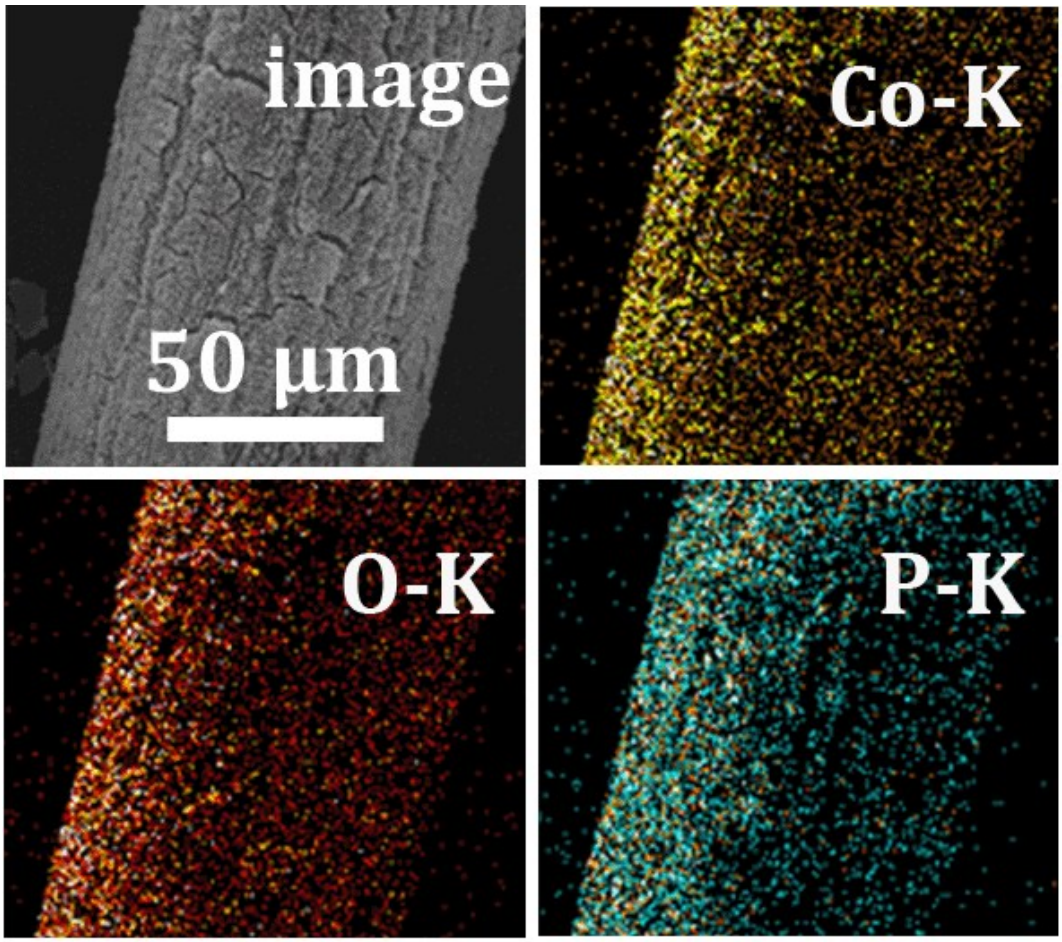

Fig. S4. Energy-dispersive X-ray (EDX) elemental mapping analysis of Co-Pi.

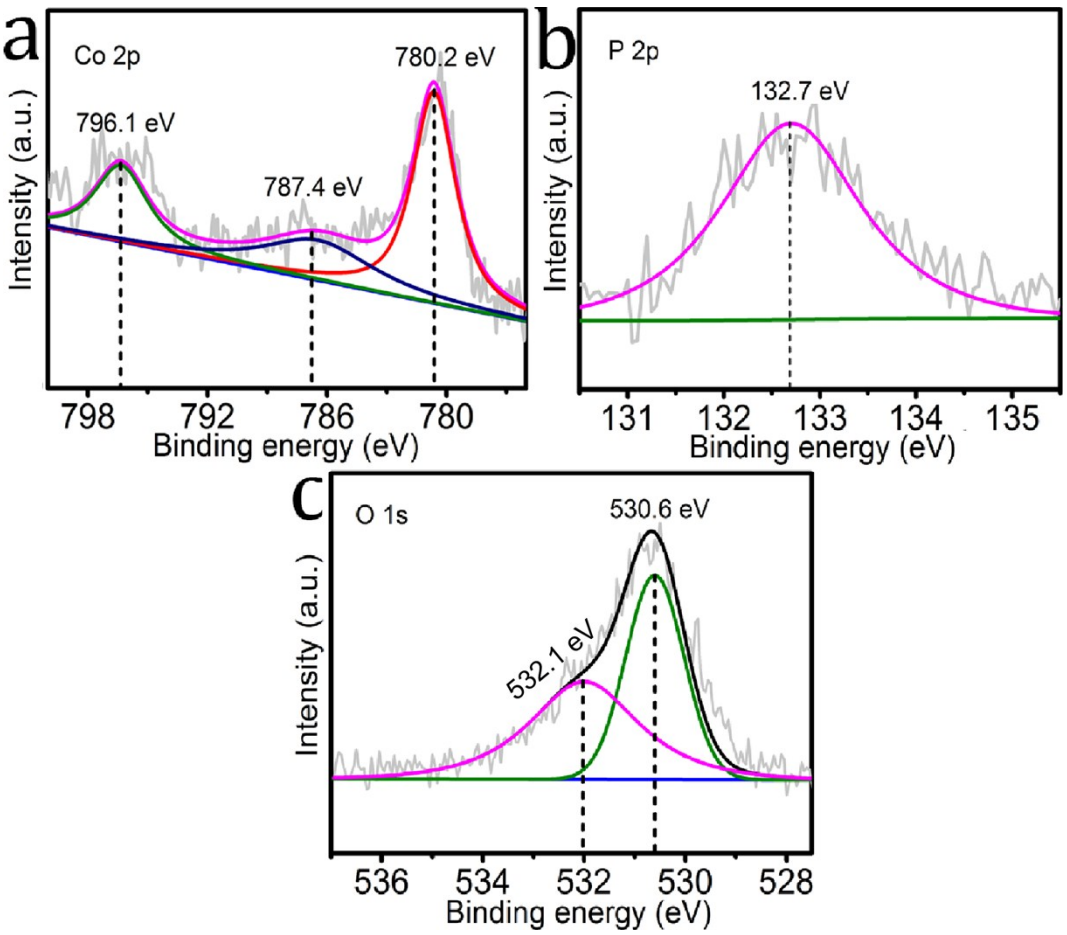

Fig. S5. XPS spectra of Co-Pi in (a) Co 2p, (b) P 2p, and (c) O 1s regions.

Table S2. Comparison of OER performance for Co-Pi/TM with other non-noble-metal electrocatalysts in neutral media.

Catalyst	j (mA cm^{-2})	η (mV)	Electrolyte (PBS)	Ref.
Co-Pi/TM	5	302	0.1 M	This work
	10	430		
	10	413	0.3 M	
	10	300	1.0 M	
Co-Pi/TM	10	450	0.1 M	19
Co-Pi/ITO	1	410	0.1 M	20
Co-Pi/FTO	0.43	420	0.1 M	21
Co-Pi/ITO	1	483	0.1 M	22
Co-Pi film	0.63	483	0.1 M	23
CoCat	1	813	0.1 M	24
NGCO	1	410	0.1 M	25
CoPi/GO	0.23	780	0.1 M	26
Fe-based film	1	480	0.1 M	27
Ni-Gly	1	480	0.5 M	28
Mn_5O_8	5	580	0.3 M	29
MnO_x	1	580	0.1 M	30
$Li_2Co_2O_4$	1	545	0.1 M	31
Co-Ni LDH	1	490	0.1 M	32
$Co(PO_3)_2$	10	590	0.1 M	33
Co_3O_4/MWNTs	1	400	0.1 M	34
Co_3S_4	3	620	0.1 M	35
Sub-MnO_x	1	420	0.3 M	36
$Mn_3(PO_4)_2$	0.32	680	0.5 M	37
$LiMnP_2O_7$	0.5	680	0.5 M	38
Cu-doped CCO	1	653	0.1 M	39
Co-W	1	420	0.05 M	40
$Co(OH)_2$	1	710	0.1 M	41

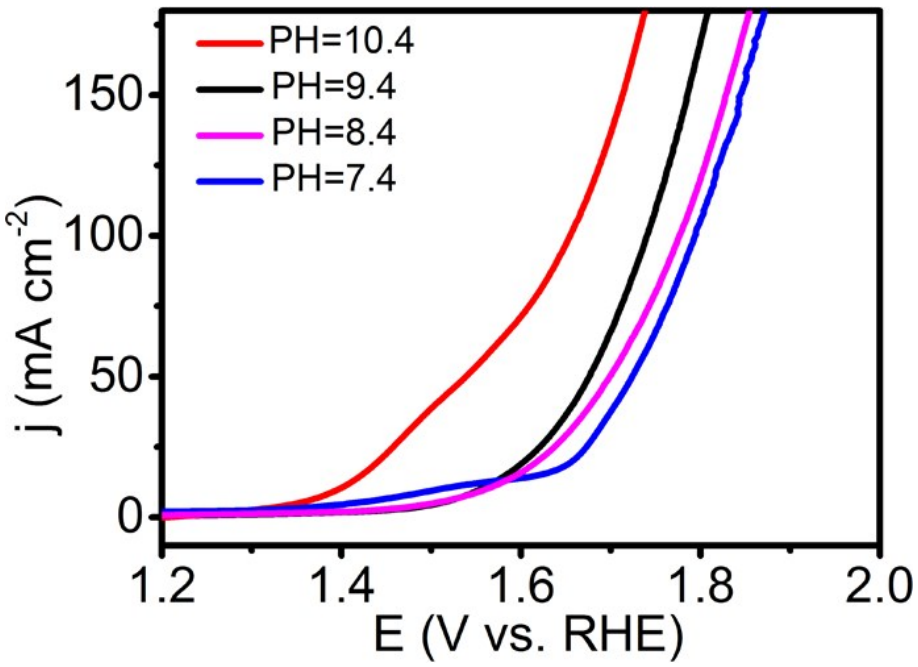

Fig. S6. LSV curves of Co-Pi/TM for OER in 1.0 M PBS with varied pH.

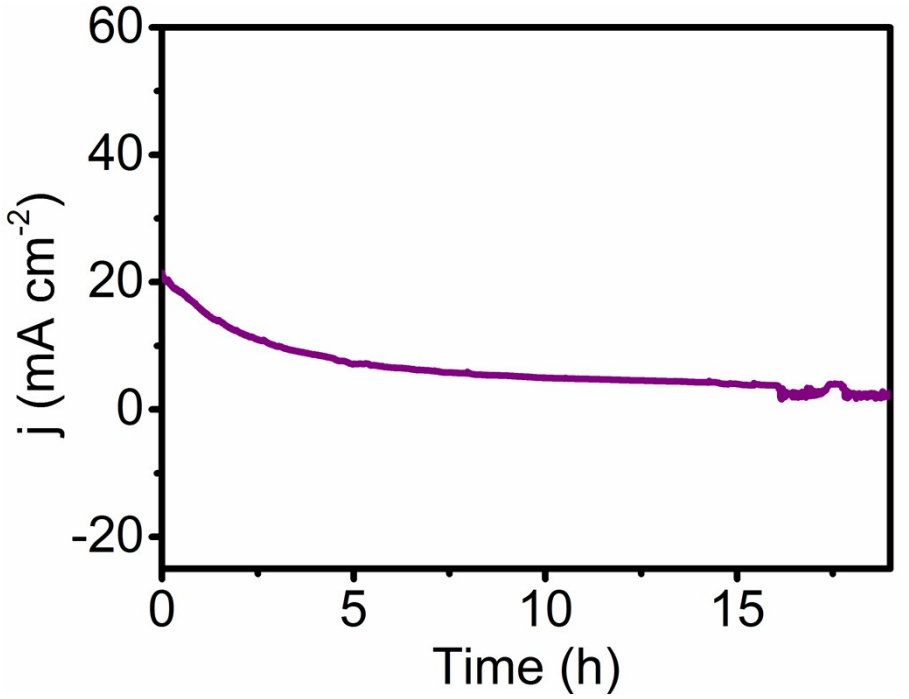

Fig. S7. Time-dependent current density curve of RuO_2/TM under static overpotential in 1.0 M PBS.

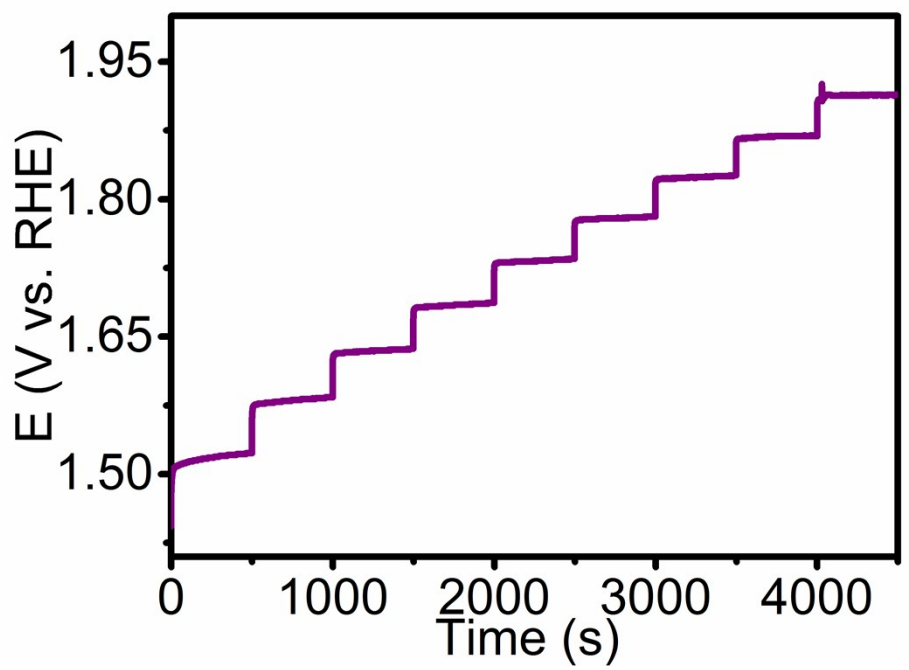

Fig. S8. Multi-current process of Co-Pi/TM in 1.0 M PBS. The current density started at 10 mA cm^{-2} and ended at 100 mA cm^{-2}, with an increment of about 10 mA cm^{-2} per 500 s without *iR* correction.

Movie S1. Overall water electrolysis at the voltage of 1.78 V employing Co_2N/TM as cathode and Co-Pi/TM as anode.

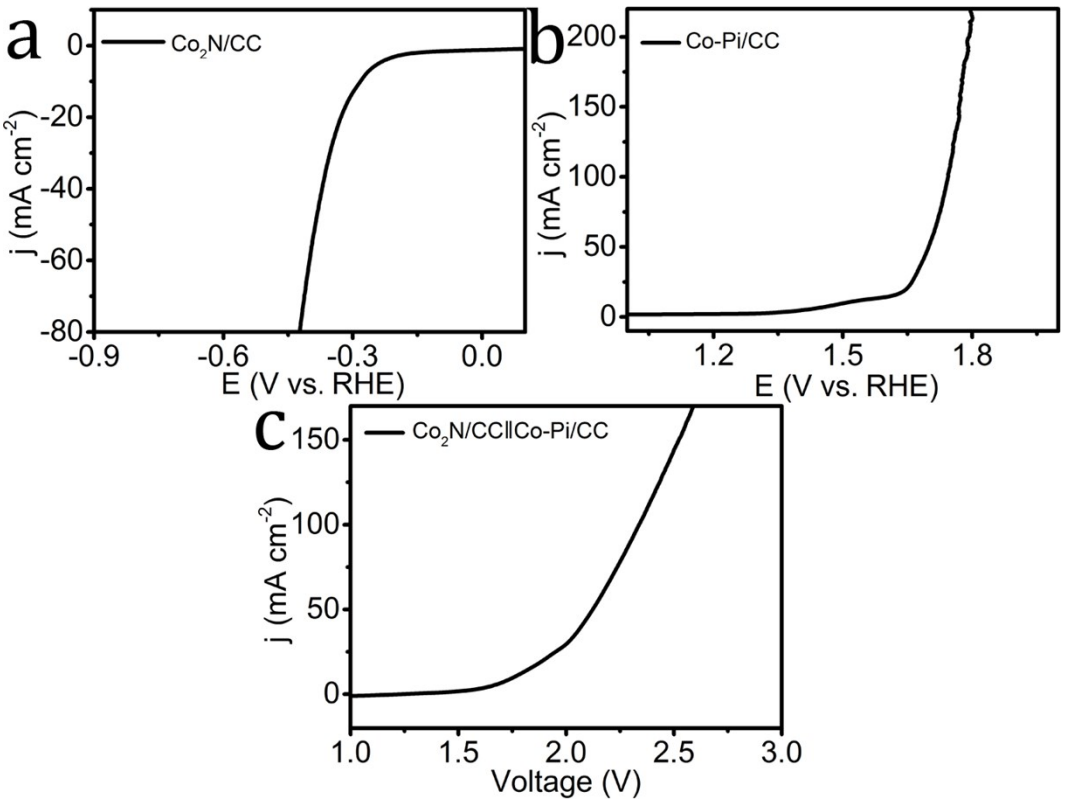

Fig. S9. Polarization curve of Co_2N/CC for (a) HER and (b) OER. (c) Polarization curve of Co_2N/CC||Co-Pi/CC for full water splitting with a scan rate of 2 mV s^{-1}. All experiments were carried out in in 1.0 M PBS.

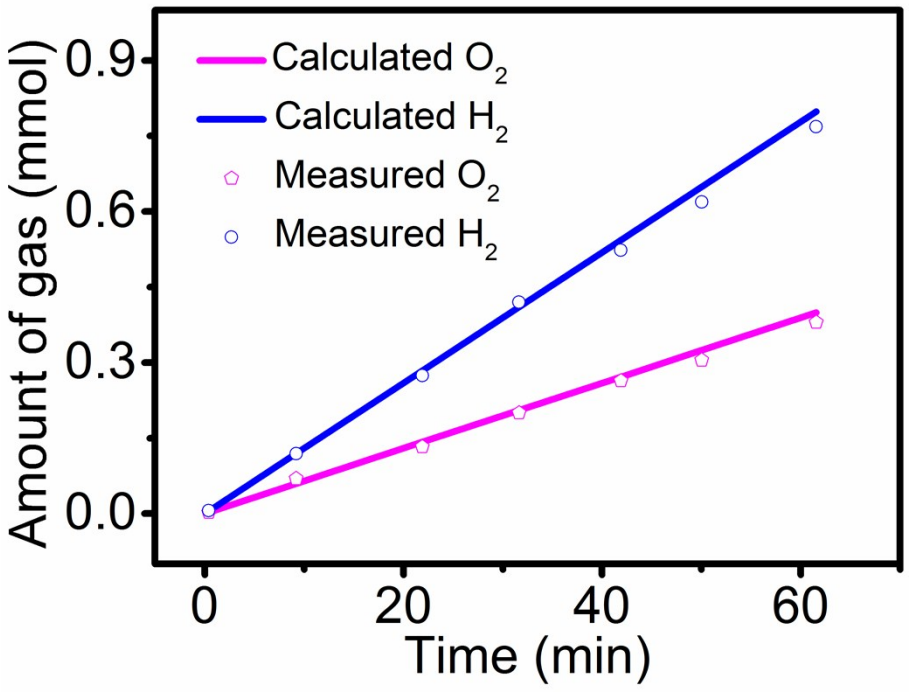

Fig. S10. The amount of gas theoretically calculated and experimentally measured vs. time for overall water splitting of Co_2N/TM||Co-Pi/TM.

References

1 J. C. Cruz, V. Baglio, S. Siracusano, V. Antonucci, A. S. Aricò, R. Ornelas, L.

Ortiz-Frade, G. Osorio-Monreal, S. M. Durón-Torres and L.G. Arriaga, *Int. J. Electrochem. Sci.,* 2011, **6**, 6607-6619.

2 G. Kresse and J. Furthmuller, *Comp. Mater. Sci.,* 1996, **6**, 15-50.

3 G. Kresse and J. Furthmuller, *Phys. Rev. B,* 1996, **54**, 11169-11186.

4 G. Kresse and J. Hafner, *Phys. Rev. B*, 1994, **49**, 14251-14269.

5 J. P. Perdew, K. Burke and M. Ernzerhof, *Phys. Rev. Lett.,* 1997, **78**, 1396-1396.

6 G. Kresse and D. Joubert, *Phys. Rev. B,* 1999, **59**, 1758-1775.

7 P. E. Blochl, *Phys. Rev. B,* 1994, **50**, 17953-17979.

8 H. J. Monkhorst and J. D. Pack, *Phys. Rev. B,* 1976, **13**, 5188-5192.

9 A. Riou, Y. Cudennec and Y. Gerault, *Acta Crystallographica C,* 1989, **45**, 1412-1413.

10 J. Shi, Z. Pu, Q. Liu, A. M. Asiri, J. Hu and X. Sun, *Electrochimica Acta,* 2015*,* **154***,* 345-351.

11 K. Li, J. Zhang, R. Wu, Y. Yu and B. Zhang, *Adv. Sci.,* 2016, **3**, 1500426.

12 S. Cobo1, J. Heidkamp, P. A. Jacques, J. Fize, V. Fourmond, L. Guetaz, B. Jousselme, V. Ivanova, H. Dau, S. Palacin, M. Fontecave and V. Artero, *Nat. Mater.,* 2012, **11**, 802-807.

13 P. D. Tran, M. Nguyen, S. S. Pramana, A. Bhattacharjee, S. Y. Chiam, J. Fize, M. J. Field, V. Artero, L. H. Wong, J. Loo and J. Barber, *Energy Environ. Sci.,* 2012, **5**, 8912-8916.

14 X. Liu, S. Cui, Z. Sun and P. Du, *Chem. Commun.,* 2015, **51**, 12954-12957.

15 X. Zou, X.Huang, A. Goswami, R. Silva, B. R. Sathe, Elis ˇka Mikmekov and Tewodros Asefa, *Angew. Chem., Int. Ed.,* 2014, **53**, 4372-4376.

16 D. Merki, H. Vrubel, L. Rovelli, S Fierro and X. Hu, *Chem. Sci.,* 2012, **3**, 2515-2525.

17 E. J. Popczun, C. G. Read, C. W. Roske, N. S. Lewis and R. E. Schaak, *Angew. Chem., Int. Ed.,* 2012, **51**, 12703-12706.

18 J. Tian, Q. Liu, A. M. Asiri and X. Sun, *J. Am. Chem. Soc.,* 2014, **136**, 7587-7590.

19 L. Xie, R. Zhang, L. Cui, D. Liu, S. Hao, Y. Ma, G. Du, A. M. Asiri and X. Sun, *Angew. Chem., Int. Ed.,* 2017*,* **129***,* 1084-1088.

20 M. W. Kanan and D. G. Nocera, *Science,* 2008, **312**, 1072-1075.

21 E. R. Young, D. G. Nocera and V. Bulović, *Energy Environ. Sci.,* 2010, **3**, 1726-1728.

22 Y. Surendranath, M. Dinca and D. G. Nocera, *J. Am. Chem. Soc.,* 2009, **131**, 2615-2620.

23 M. W. Kanan, J. Yano, Y. Surendranath, M. Dincă, V. K. Yachandra and D. G. Nocera, *J. Am. Chem. Soc.,* 2010, **132**, 13692-3701.

24 D. González-Flores, I. Sánchez, I. Zaharieva, K. Klingan, J. Heidkamp, P. Chernev, P. W. Menezes, M. Driess, H. Dau and M. L. Montero, *Angew. Chem., Int. Ed.,* 2015, **54**, 2472-2476.

25 A. Vasileff, S. Chen and S. Qiao, *Nanoscale Horiz.,* 2016, **1**, 41-44.

26 J. Tian, H. Li, A. M. Asiri, A. O. Al-Youbi and X. Sun, *Small,* 2013, **9**, 2709-2714.

27 Y. Wu, M. Chen, Y. Han, H. Luo, X. Su, M. Zhang, X. Lin, J. Sun, L. Wang, L. Deng, W. Zhang and R. Cao, *Angew. Chem., Int. Ed.,* 2015, **54**, 4870-4875.

28 D. Wang, G. Ghirlanda and J. P. Allen, *J. Am. Chem. Soc.,* 2014, **136**, 10198-10201.

29 D. Jeong, K. Jin, S. E. Jerng, H. Seo, D. Kim, S. H. Nahm, S. H. Kim and K. T. Nam, *ACS Catal.,* 2015, **5**, 4624-4628.

30 I. Zaharieva, P. Chernev, M. Risch, K. Klingan, M. Kohlhoff, A. Fischer and H. Dau, *Energy Environ. Sci.,* 2012, **5**, 7081-7089.

31 G. P. Gardner, Y. B. Go, D. M. Robinson, P. F. Smith, J. Hadermann, A. Abakumov, M. Greenblatt and G. C. Dismukes, *Angew. Chem., Int. Ed.,* 2012, **51**, 1616-1619.

32 Y. Zhang, B. Cui, C. Zhao, H. Lin and J. Li, *Phys. Chem. Chem. Phys.,* 2013, **15**, 7363-7369.

33 H. S. Ahn and T. D. Tilley, *Adv. Funct. Mater.,* 2013, **23**, 227-233.

34 J. Wu, Y. Xue, X. Yan, W. Yan, Q. Cheng and Y. Xie, *Nano Res.,* 2012, **5**, 521-530.

35 Y. Liu, C. Xiao, M. Lyu, Y. Lin, W. Cai, P. Huang, W. Tong, Y. Zou and Y. Xie,

Angew. Chem., Int. Ed., 2015, **54**, 11231-11235.

36 K. Jin, A. Chu, J. Park, D. Jeong, S. E. Jerng, U. Sim, H. Y. Jeong, C. W. Lee, Y. S. Park, K. D. Yang, G. K. Pradhan, D. Kim, N. E. Sung, S. H. Kim and K. T. Nam, *Sci. Rep.,* 2015, **5**, 10279.

37 K. Jin, J. Park, J. Lee, K. D. Yang, G. K. Pradhan, U. Sim, D. Jeong, H. L. Jang, S. Park, D. Kim, N. E. Sung, S. H. Kim, S. Han and K. T. Nam, *J. Am. Chem. Soc.,* 2014, **136**, 7435-7443.

38 J. Park, H. Kim, K. Jin, B. J. Lee, Y. S. Park, H. Kim, I. Park, K. D. Yang, H. Y. Jeong, J. Kim, K. T. Hong, H. W. Jang, K. Kang and K. T. Nam, *J. Am. Chem. Soc.,* 2014, **136**, 4201-4211.

39 Y. Zhang, B. Cui, O. Derr, Z. Yao, Z. Qin, X. Deng, J. Li and H. Lin, *Nanoscale,* 2014, **6**, 3376-3383.

40 B. Zhang, X. Wu, F. Li, F. Yu, Y. Wang and L. Sun, *Chem. Asian J.,* 2015, **10**, 2228-2233.

41 Y. Zhang, B. Cui, Z. Qin, H. Lin and J. Li, *Nanoscale,* 2013, **5**, 6826-6833.